Original Article

Magnetic Resonance Neurography of the Brachial Plexus Using 3D SHINKEI: Comparative Evaluation with Conventional Magnetic Resonance Sequences for the Visualization of Anatomy and Detection of Nerve Injury at 1.5T

Prashant Prabhakaran Nair, Yogesh K. Mariappan[1], Samir M. Paruthikunnan, Asha Kamath[2], Narayana K. Rolla[1], Indrajit Saha[3], Rajagopal Kadavigere

Department of Radiodiagnosis and Imaging, Kasturba Medical College Manipal, Manipal Academy of Higher Education, [1]Philips India Ltd., Bengaluru, Karnataka, India, [2]Department of Statistics, Prasanna School of Public Health, Manipal Academy of Higher Education, [3]Philips India Ltd., Gurgaon, Haryana, India

Abstract

Background and Purpose: This work aims at optimizing and studying the feasibility of imaging the brachial plexus at 1.5T using 3D nerve-SHeath signal increased with INKed rest-tissue RARE imaging (3D SHINKEI) neurography sequence by comparing with routine sequences. **Materials and Methods:** The study was performed on a 1.5T Achieva scanner. It was designed in two parts: (a) Optimization of SHINKEI sequence at 1.5T; and (b) Feasibility study of the optimized SHINKEI sequence for generating clinical quality magnetic resonance neurography images at 1.5T. Simulations and volunteer experiments were conducted to optimize the T2 preparation duration for optimum nerve-muscle contrast at 1.5T. Images from the sequence under study and other routine sequences from 24 patients clinically referred for brachial plexus imaging were scored by a panel of radiologists for diagnostic quality. Injury detection efficacy of these sequences were evaluated against the surgical information available from seven patients. **Results:** T2 preparation duration of 50 ms gives the best contrast to noise between nerve and muscle. The images of 3D SHINKEI and short-term inversion recovery turbo spin-echo sequences are of similar diagnostic quality but significantly better than diffusion weighted imaging with background signal suppression. In comparison with the surgical findings, 3D SHINKEI has the lowest specificity; however, it had the highest sensitivity and predictive efficacy compared to other routine sequences. **Conclusion:** 3D SHINKEI sequence provides a good nerve–muscle contrast and has high predictive efficacy of nerve injury, indicating that it is a potential screening sequence candidate for brachial plexus scans at 1.5T also.

Keywords: Diffusion-weighted imaging with background signal suppression, MSDE, SHINKEI, short-term inversion recovery, T2prep

Received on: 16-01-2021 **Review completed on:** 24-05-2021 **Accepted on:** 27-05-2021 **Published on:** 08-09-2021

Introduction

The brachial plexus is a network of nerves that normally begin as five ventral roots of the C5, C6, C7, C8, and T1 spinal nerves. The C5 and C6 roots combine to form the upper trunk, the C7 root continues as the middle trunk and the C8 and T1 roots combine to form the lower trunk. Each of the trunks forms anterior and posterior divisions that finally form three cords,[1] though there may be variants.[2,3] The peripheral nerves originating from the brachial plexus innervate the muscles of the thorax and the upper extremities and have sensory innervations to the skin of the shoulder and arms.[1] The brachial plexus is an injury-prone anatomy and is involved in a variety of pathologies leading to impaired

Access this article online

Quick Response Code:

Website: www.jmp.org.in

DOI: 10.4103/jmp.JMP_13_21

Address for correspondence: Dr. Rajagopal Kadavigere, Department of Radiodiagnosis and Imaging, Kasturba Medical College, Manipal Academy of Higher Education, Manipal 576 104, Karnataka, India. E mail: rajarad@gmail.com

How to cite this article: Nair PP, Mariappan YK, Paruthikunnan SM, Kamath A, Rolla NK, Saha I, *et al.* Magnetic resonance neurography of the brachial plexus using 3D SHINKEI: Comparative evaluation with conventional magnetic resonance sequences for the visualization of anatomy and detection of nerve injury at 1.5T. J Med Phys 2021;46:140-7.

upper limb functions.[4] Sixty-seven percent of closed brachial plexus trauma is caused by motorcycle accidents followed by car crashes (14%). Among these, 53% of the injuries are complete, 39% are limited to the upper plexus, and 6% limited to the lower plexus alone.[5] Obstetric brachial plexus injury during labor is also common.[6]

Conventional techniques to image the brachial plexus include the ultrasound and the magnetic resonance imaging (MRI). Ultrasound requires thorough knowledge of the anatomy[7] and is operator dependent. With conventional MR methods, the oblique course of these nerves, presence of blood vessels, and musculature make the brachial plexus extremely difficult to image. The nerve visualization with high conspicuity is obtained through nonneural tissue suppression by heavy T2 weighting;[8] however, these techniques often fail to suppress the signal from the small blood vessels intertwining the fine nerves. Fat suppressed inversion recovery turbo spin-echo (TSE) sequence is useful to image peripheral nerves,[9] however, due to low signal-to-noise ratio (SNR) coupled with only partial suppression of the blood vessels, the delineation of the nerves may not be easy.[10] As a result of this, MR neurography,[8] a broad and actively evolving domain for imaging and evaluation of the peripheral nerves, has generated considerable interest among clinicians and researchers.[8-12] Nowadays, this technique is optimized usually at 3T. Diffusion-weighted imaging with background signal suppression (DWIBS) based MR neurography[13,14] with maximum intensity projection (MIP) makes possible the visualization of the whole nerve along its long axis. However, relatively lower spatial resolution is often a challenge to its clinical efficacy to visualize fine nerves and to detect focal lesions.[15] Another diffusion technique that is clinically feasible to study infiltration and disruption of the plexuses is tractography with diffusion tensor imaging.[16]

Three-dimensional nerve-SHeath signal increased with INKed rest-tissue RARE imaging (3D SHINKEI) MR neurography sequence utilizes three components: Firstly, a spectral adiabatic inversion recovery fat suppressing prep-pulse. Secondly, an improved motion-sensitized driven equilibrium iMSDE prep-pulse, which retains signal from the static and high T2 tissues while that from the moving blood tissues and low T2 background is suppressed [Figure 1]. Thirdly, a 3D volume isotropic acquisition (VISTA) acquisition with low refocusing flip angle evolution designed for targeting nerves.[13,17,18] With the fat and moving blood signal suppression, this sequence generates high-quality nerve images with an improved resolution at the high field MR.[8,19] To obtain high nerve SNR, most of the recent developments have happened at 3.0T MRI.[10,12,20] MRI sequence is usually rated based on its ability to locate the trauma, nerve continuity, compressions, and disruptions.[21,22] A recent study on brachial plexus imaging concluded that although the nerve signal is better at 3T, the diagnostic quality of the images did not differ significantly from that of 1.5T.[20]

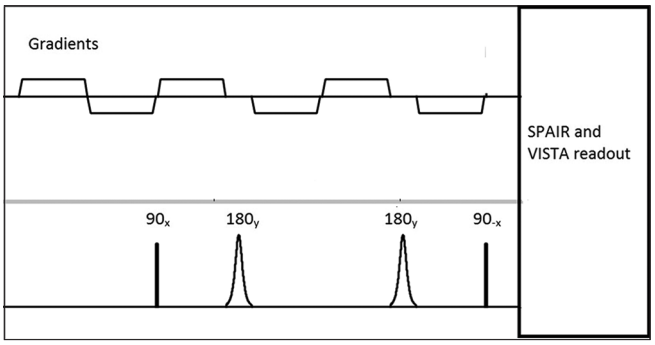

Figure 1: iMSDE preparation module. Gradients shown are applied in the direction in which the motion sensitization is desired. $T2_{prep}$ is the MSDE duration that also contributes to an additional T2 contrast. In the SHeath signal increased with INKed rest-tissue RARE imaging sequence, this is followed by a fat suppressing spectral adiabatic inversion recovery pulse

We hypothesize that with an experimentally optimized T2 prep pulse sequence, optimum nerve signal, and nerve-to-muscle contrast resolution could be obtained using 1.5T. Hence, we argue for the importance of continued research at 1.5T, considering that a very high share of clinical MRI scanners is still 1.5T. In this study, we compare the diagnostic efficiency of 3D SHINKEI MR neurography sequence over the conventional 2D short-term inversion recovery (STIR) TSE imaging sequence and DWIBS in imaging patients to predict nerve root injury of brachial plexus at 1.5T.

We conducted this study to optimize and study the feasibility to obtain diagnostic quality images with 3D SHINKEI sequence at 1.5T MRI. For this, we followed an experimental study on volunteers followed by the feasibility on 24 patients. The grading was decided based on nerve SNR, blood signal suppression, robust fat suppression, appreciation of the nerve signal proximally and distally, signal spread in fine nerve.

Materials and Methods

Institutional Ethical Committee approval was obtained for the study. Prior written informed consent was obtained before the scans from all the enrolled subjects. The study was performed in two parts: (a) Optimization of T2prep sequence at 1.5T; and (b) feasibility study of the optimized SHINKEI sequence for generating high-quality MR Neurography images and its comparison with DWIBS MR Neurography and 2D STIR TSE.

Optimization of $T2_{prep}$ of SHINKEI

One of the primary goals of this work was to find the optimal preparation duration of the iMSDE module of the SHINKEI sequence at 1.5T so that the muscle signal is suppressed as much as possible while retaining the nerve signal (S_{nerve}). Numerical simulations of the iMSDE module's $T2_{prep}$ with durations in the range of 0-100 ms acquisition were performed. Signal for a tissue at the end of the module was evaluated based on the simplistic T2 decay model (equation 1).

$$Sprep = \exp\left(\frac{T2prep}{T2}\right) \quad (1)$$

The nerve-muscle contrast (equation2) has to be maximized.

$$C_{nerve-muscle} = S_{nerve} - S_{muscle} \quad (2)$$

$C_{nerve-muscle}$ is a good measure for a tradeoff to suppress the muscle background while retaining maximum nerve signal. The T2 values for nerve and muscle at 1.5T were taken as 74 ms and 35 ms, respectively.[22,23] The proton density was assumed to be the same for nerve and muscle. The behavior of S_{nerve} and the $C_{nerve-muscle}$ was then investigated with respect to the iMSDE preparation duration.

In vivo volunteer imaging

All experiments were performed on a 1.5 T MR Scanner (Achieva, Philips, Best, The Netherlands) using a 16 channel-head and neck NV SENSE coil. A low constant refocusing angle of 30° was employed for the VISTA acquisition.

In vivo MR neurography data obtained with a range of iMSDE durations (30, 40, 50, 60, and 70 ms) from a set of seven volunteers (one female and six males with mean age of 25.43 ± 2.82) and the results from the numerical simulation were compared to mean normalized signal from the volunteers. The mean nerve signal was measured with an elliptical area of 10 mm^2, the muscle signal (mean) with a rectangular area of 100 mm^2, and the air (noise– standard deviation) with an area of 800 mm^2 [Figure 2c]. Experimental and theoretical values for the signal-to-noise ratio and contrast resolution were compared. Furthermore, the best placement of a shim volume was experimentally determined for robust background fat suppression.

Relevant sequence parameters were:-SHINKEI: Repetition time (TR) of 2.5 s, effective echo time: 127 ms, echo train length: 80, with a low constant refocusing flip angles (alpha = 30°) isometric voxel: 1.2 mm, acquisition matrix: 208 × 312, Velocity encoding: 1 cm/s with a scan time of 5:27 min. DWIBS: Repetition time: 9 s, echo time: 72 ms, b factor: 600 s/mm^2, EPI factor: 43, signal averages: 20, voxel size: 1.39 × 1.39 × 3 mm, acquisition matrix: 132 × 97, and a scan time of 5:32 min. 2D STIR: Repetition time: 2.5 s, echo time: 80 ms, echo train length: 19, signal averages: 1, acquisition matrix: 276 × 158, and a scan time of 4:20 min.

SHINKEI Feasibility Study

Subjects

Most of the cases involved brachial plexopathies secondary to trauma ($n = 13$), previous surgery ($n = 3$), Neurofibroma ($n = 1$), cervical radiculopathy ($n = 1$). Six patients were referred to brachial plexus due to pain or numbness in the upper arm and three of the cases were normal MRI of the brachial plexus. One patient was a 30-year-old female. The rest were males in the age range 17-65. Further clinical details of each patient is given in Supplementary Table 1.

The optimized SHINKEI sequence was performed along with the routine protocol in 24 patients clinically advised for brachial plexus imaging. The diagnostic quality of SHINKEI, STIR, and DWIBS images for different locations– preganglionic and postganglionic brachial plexus was rated on a four-point scale (4 – excellent, 3 – good, 2 – moderate, and 1 – poor) for diagnostic confidence by a panel of two experienced radiologists, RK and SM, with 20 and 11 years of experience, respectively, through consensus.

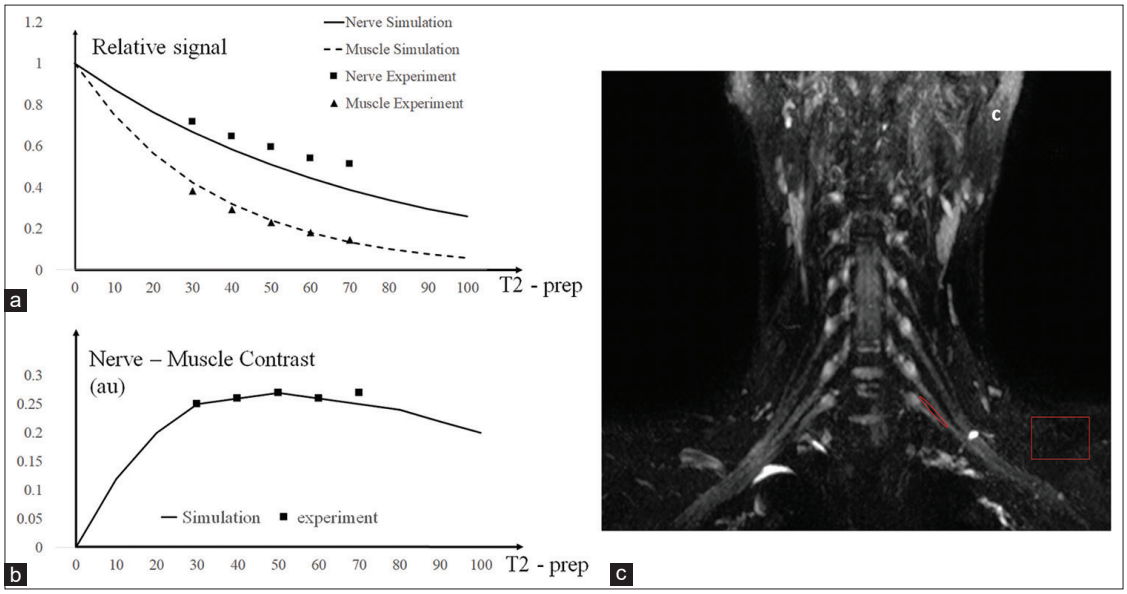

Figure 2: (a) The exponential decay of the nerve and muscle signal. Simulation values and experimental relative signal values from nerve and muscle after normalization are depicted. (b) The cost function Nerve- Muscle contrast; Experimental validation of iMSDE optimization in comparison to the theoretical values. The nerve-muscle contrast peaks at $T2_{prep}$ time of 50 ms. iMSDE $T2_{prep}$ time is hence chosen as 50 ms. (c) Visualization of the anatomy of the brachial plexus in a 24-year-old volunteer with maximum intensity projection images. The oval and square ROIs indicate how the nerve and background SNR is measured

The image quality aspects considered while scoring were blood signal suppression, robust fat suppression, appreciation of the nerve signal proximally and distally, and signal spread in fine nerve. An objective comparison of the SHINKEI and STIR images was performed by measuring the SNR and contrast ratios on the contralateral side of the patient. It was not possible to perform the objective analysis on the DWIBS images as spatial resolution of the images was poor, the nerve structures blurred. One out of the 24 patients had to be excluded from this analysis as the plexopathy was bilateral. In addition, these data were also compared to the surgical findings available in seven of the 24 patients to check the accuracy for preoperative detection of nerve injury.

Statistical analysis

Intraclass correlation was employed to evaluate the reliability of the readers. Nonparametric Friedman test for the repeated measures was conducted for the grades (arrived by consensus) for the different sequences, and a $P < 0.05$ was considered statistically significant. Wilcoxon signed-rank tests with Bonferroni corrections ($P = 0.016$) were performed for *post hoc* test. A two-tailed paired *t*-test was performed to compare the nerve SNR and the nerve–muscle contrast ratios of SHINKEI and the STIR TSE images. Chi-square test was performed to compare the predictive potential of SHINKEI, STIR TSE, and DWIBS with regard to avulsion (with Yates corrected *P* values). A Goodman–Kruskal index of predictive association (lambda) was arrived at using this data. All statistical tests were performed using IBM SPSS (SPSS, Version 26.0. Bangalore).

Results

Optimization of iMSDE preparation module

The numerical simulation indicates that the S_{nerve} and S_{muscle} decrease exponentially characteristic of their T2 relaxation rates [Figure 2a] and $C_{nerve\text{-}muscle}$ peaked at iMSDE $T2_{prep}$ time 50 ms [Figure 2b], and the experimental data obtained from the volunteers followed the trends [Figure 2a and b]. Based on this, a $T2_{prep}$ of 50 ms was chosen as the best tradeoff and nerve signal for the feasibility study of the optimized SHINKEI sequence for generating high-quality MRN images at 1.5T [Figure 2c]. A shim volume partly extending to the neck and partly to the thorax and not including space outside the subject was the best for robust fat suppression.

Feasibility study of SHINKEI

A comparative evaluation based on the consensus grades is graphically represented as a bar chart in Figure 3. The results [Table 1] of the Intraclass correlation between the two readings are reported as ICC (95% Confidence Interval), *P* value for the three sequences at different anatomical locations of the brachial plexus. The independent scores from each radiologist are given in Supplementary Tables 2 and 3.

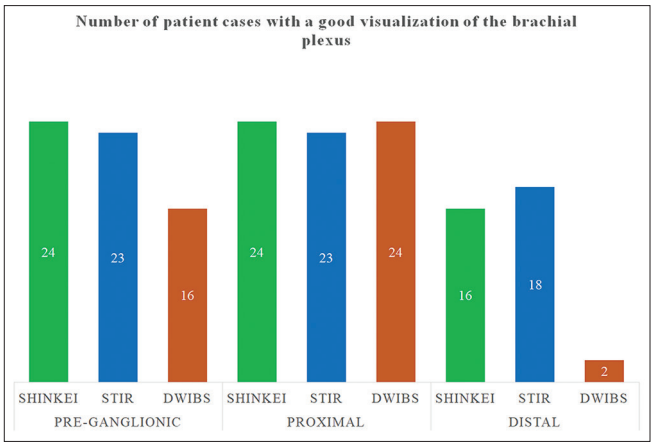

Figure 3: A comparison between SHeath signal increased with INKed rest-tissue RARE imaging, short-term inversion recovery turbo spin-echo and diffusion-weighted imaging with background signal suppression image quality based on grading at various anatomical regions of the brachial plexus. The bars indicate the number of cases where a particular anatomical region has obtained a high score of 3 on 4 ("good" to "excellent" visualization)

Table 1: Results of intra class correlation coefficient used to assess the reliability of the readers

	Preganglionic plexus	Postganglionic roots	
		Proximal	Distal
SHINKEI	0.869, *P*<0.001	0.785, *P*<0.001	0.790, *P*<0.001
STIR	0.889, *P*<0.001	0.747, *P*<0.001	0.968, *P*<0.001
DWIBS	0.719, *P*<0.001	0.713, *P*<0.001	0.794, *P*<0.001

SHINKEI: SHeath signal increased with INKed rest-tissue RARE Imaging, STIR: Short-term inversion recovery, DWIBS: Diffusion-weighted imaging with background signal suppression

The Friedman test and the corresponding Wilcoxon nonparametric test showed that the readings were not significantly different for SHINKEI and STIR throughout the entire anatomy. However, SHINKEI and STIR were considerably better than DWIBS ($P = 0.002$ each) at the preganglionic plexus and the distal postganglionic plexus ($P < 0.001$ each). At the level of the roots, there was no significant difference in the readings.

Preganglionic plexus

Mean ranks (Median (25^{th} percentile and 75^{th} percentile)) for SHINKEI is 2.5 (4, [4, 4]), STIR is 2.1 (4, [3,4]) and DWIBS is 1.4 (3, [2, 3]). Chi-Square 16.9, df 2, $P = 0.0002$. *Post hoc* test: No significant difference between the SHINKEI and STIR scores ($P = 0.02$), both SHINKEI ($P = 0.0002$) and STIR ($P = 0.0021$) significantly better than DWIBS.

Postganglionic proximal (Roots and trunks)

Mean ranks (25^{th} percentile, 50^{th} percentile, 75^{th} percentile) for SHINKEI 2.3 (4, [4, 4]), STIR 1.8 (4, [3, 4]) and DWIBS 1.9 (4, [3, 4]). Chi-Square 2.44, df 2, $P = 0.295$. There was no significant difference between SHINKEI, DWIBS, and STIR TSE scores.

Postganglionic distal (divisions and cords): Mean ranks (Median (25th percentile, 75th percentile)) for SHINKEI 2.3 (3, [3, 4]), STIR 2.5 (3, 3,4) and DWIBS 1.3 (2, [2,3]). Chi-Square 21, df 2, $P < 0.0001$. *Post hoc* test: No significant difference between the SHINKEI and STIR scores ($P = 0.1499$), both SHINKEI ($P = 0.0004$) and STIR ($P = 0.0002$) significantly better than DWIBS.

Objective analysis of SHINKEI and STIR TSE images

The mean nerve SNR of the SHINKEI images was greater than on the short term inversion recovery (STIR) turbo spin-echo (TSE) images (78.52 vs. 65.48 au., $P < 0.001$). The nerve–muscle contrast ratio of the SHINKEI images was greater than the STIR TSE images (0.61 vs. 0.37 au., $P < 0.001$).

In addition, for patients, the extent of the avulsion and ruptures were better appreciated on the SHINKEI image compared to the DWIBS [Figures 4 and 5]. SHINKEI images depicted the diffusion restriction at the neuroma formation clearly [Figure 6]. The grade 1 subacute injury is clearly discernible on the SHINKEI and STIR TSE images but not on the DWIBS images [Figure 7]. Nineteen nerve roots were identified in surgery from the seven patients. The results including sensitivity, specificity, and estimated probability of correct detection were compared between the three sequences [Table 2]. In five of these patients, root avulsion was detected, and these were reflected in the imaging findings as pseudomeningioceles. This is detailed in Supplementary Table 4.

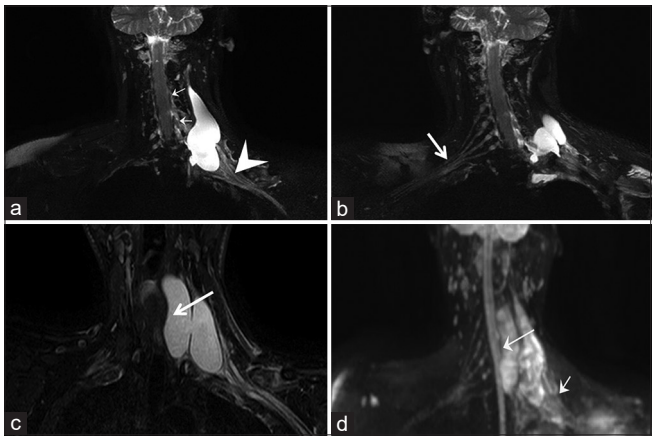

Figure 4: A 29-year-old male following road traffic accident shows root avulsions at left C5, C6, C7 and C8 levels. (a) SHINKEI shows root avulsion at C5 to C8 (arrows) and distorted distal plexus (small arrows) compared to the normal right side (b). Short-term inversion recovery turbo spin echo (c) and diffusion-weighted imaging with background signal suppression (d) for comparison

Discussion

The present study has explored the feasibility of imaging the brachial plexus with 3D SHINKEI at 1.5 T and compared it with the current clinical pulse sequences STIR and DWIBs. One of the main goals of this study was to find the optimal preparation duration of the iMSDE pulse in SHINKEI MRN that would suppress the signal from muscle while retaining most of the nerve signal. A numerical simulation that calculates the relative signal available as a function of the $T2_{prep}$ was performed, and the optimum $T2_{prep}$ for maximum nerve-muscle contrast measured through this simulation was validated with volunteer studies. Our simulation experiments with iMSDE module are in agreement with a previous study[23] that indicated the possibility of a $T2_{prep}$ pulse-set to manipulate the T2 contrast of SHINKEI. Based on the study, $T2_{prep}$ duration of 50 ms was chosen to be optimal to obtain the best contrast resolution while still ensuring good nerve signal.

The feasibility study of using SHINKEI sequence as a part of the routine neurography protocol on 24 patients at 1.5T showed that the SHINKEI sequence efficiently suppresses the background flowing blood signal and muscle signal. SHINKEI can detect avulsion, denervation changes in the muscle, and neuroma associated with brachial plexopathies better compared to the DWIBS. SHINKEI provides a better visualization of the small nerves such as suprascapular nerve. SHINKEI offers better detection of mild Grade 1 hyperintensities) and diagnoses early nerve injuries to guide further conservative management, where clinical examinations and conventional MRI sequences fail. The nerve SNR in the SHINKEI images was found to be significantly higher in comparison to the STIR TSE images. The nerve–muscle contrast ratio was found to be significantly greater on the SHINKEI images in comparison to the STIR TSE images. This could be attributed to the optimized IMSDE prep pulse that suppresses the low T2 muscle tissues. It is also to be noted that the objective analysis was not performed on the DWIBS images due to low spatial resolution.

Table 2: Comparison of potential correct prediction capability and their correlation with the surgical findings

	SHINKEI	STIR	DWIBS
Sensitivity (%)	88	75	37.5
Specificity (%)	67	100	100
Accuracy (%)	84	79	47.3
Yates corrected *P* (Chi-square test done on data): Difference from surgery observations	0.03* Chi-square - 4.46	0.01* Chi-square - 6.11	0.2 Chi-square - 1.64
Goodman-Kruskal index of predictive association (lambda) Estimated probability of correct prediction (without knowing surgical results a-priori) (%)	78	67	52

*Statistically significant correlation with surgical findings. SHINKEI: SHeath signal increased with INKed rest-tissue RARE Imaging, STIR: Short-term inversion recovery, DWIBS: Diffusion-weighted imaging with background signal suppression

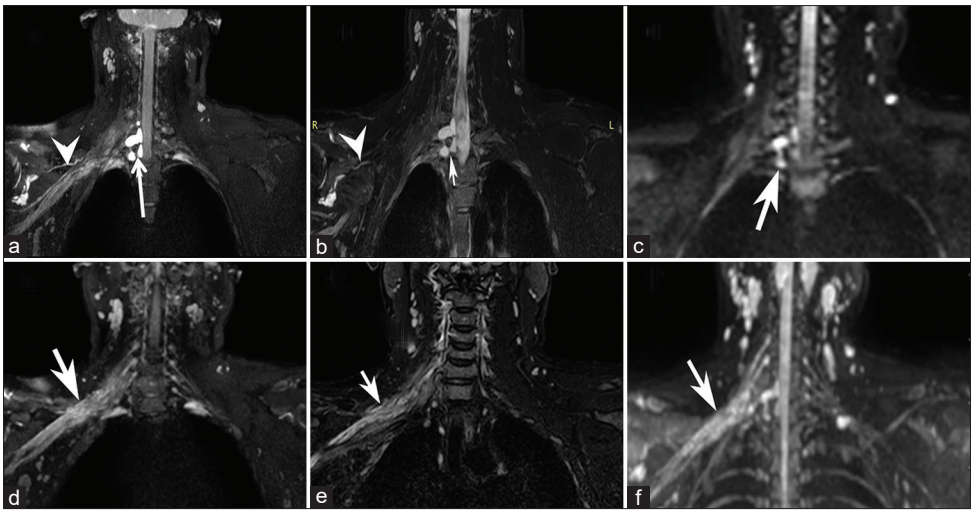

Figure 5: A 22 year old male with RTA: SHeath signal increased with INKed rest tissue RARE imaging (a and d), short term inversion recovery (b and e) and diffusion weighted imaging with background signal suppression (c and f) show lower root avulsion with pseudomeningioceles (arrows); SHeath signal increased with INKed rest tissue RARE imaging and short term inversion recovery show hyperintensity in the suprascapular nerve (arrowhead, a and b), which was not appreciated in the diffusion weighted imaging with background signal suppression (c). Distal nerve injury is better depicted in SHINKEI and short term inversion recovery sequence

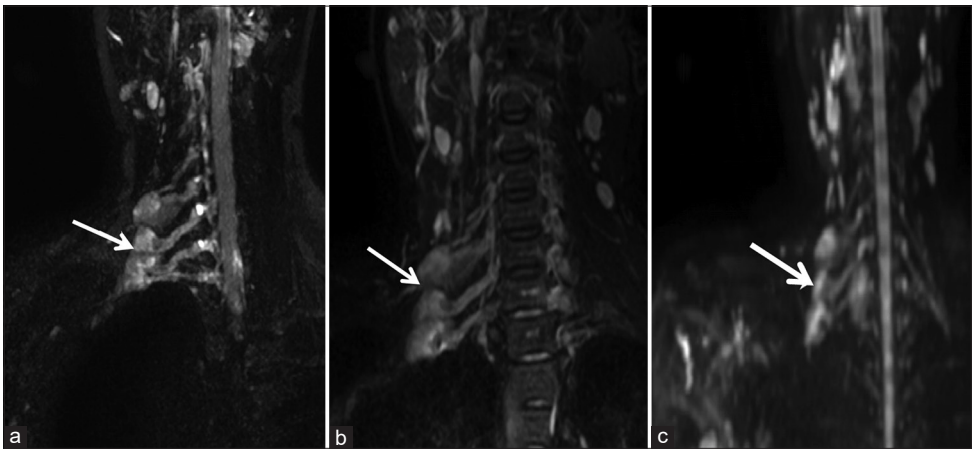

Figure 6: A 30-year-old female with transection of the right roots and trunks of brachial plexus with neuroma formation, better appreciated in the SHeath signal increased with INKed rest-tissue RARE imaging (a) and short-term inversion recovery (b) images compared to the diffusion weighted imaging with background signal suppression (c). Nerve conduction study findings were correlating with the imaging findings

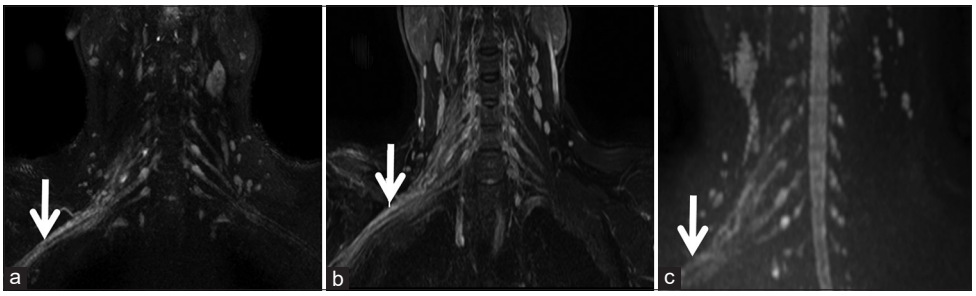

Figure 7: A 35 year old male patient with injury to right distal brachial plexus. The grade 1 sub acute injury is discernible on the SHeath signal increased with INKed rest tissue RARE imaging (a) and the short term inversion recovery as hyperintensities (white arrows) (b) and is not well appreciated in diffusion weighted imaging with background signal suppression image (c)

Of the seven patients where surgery was performed, SHINKEI sequence had a higher sensitivity in diagnosing preganglionic trauma, and higher accuracy in predicting the outcome. However, the specificity of the SHINKEI sequence was marginally lower than the STIR TSE sequence. SHINKEI along with the routine sequences has a higher potential for being a

screening sequence for predicting preganglionic nerve trauma. One of the limitations to be noted is that this cross-validation was done only on 19 nerve roots from these seven patients.

The scores at distal nerves, where the size of the nerves is subvoxel, are not satisfactory due to blurring. This could be attributed to signal-spread due to intravoxel off-resonance effects due to the lower refocusing flip angles of the VISTA. These effects are mentioned in a lumbar plexus imaging study.[24] We plan to take this study forward by incorporating the off-resonance effects for the optimization of signal-spread in our VISTA model and validating the same. To make the SHINKEI sequence at 1.5T more "nerve tissue specific" with higher S_{nerve} by dephasing the moving spins, optimization of the refocusing pulse train modulation of the VISTA acquisition can be useful.[24,25] It was observed that the blood and muscle signal suppression was effective in normal subjects with both SHINKEI and DWIBS sequences. However, in case of severe trauma, areas of soft-tissue injury with possible hemorrhage at the site of trauma were not well suppressed with SHINKEI. This limitation is partly overcome by generating the MIPs and viewing the same in the desired direction. The T2 preparation can be made more robust at the neck–thorax junction by applying the iMSDE module based on a BIR-4 pulse.[26]

Our study indicates that improper fat signal suppression could affect the nerve visualization with on the SHINKEI images, a problem that could be overcome with a proper shim volume placement as described in the result. Another artifact that would affect the nerve visualization is unsuppressed blood signal in the case of hemorrhage following trauma. In this case, the SHINKEI sequence with the iMSDE velocity encoding and the MIP performs better compared to the DWIBS and the STIR TSE sequences. Finally, from our study, we find that the visualization of the thin nerves of the distal plexus appears blurred. This is probably due to the nerve structures being subvoxel size and them being embedded in muscle tissue, hence undergoing signal spread. This is a problem to be addressed in future.

Conclusion

This study establishes the optimum value for T2prep for the best nerve–muscle contrast at 1.5T imaging to be 50 ms. Compared to 2D acquisitions, the coronal 3D SHINKEI acquisition ensured that the nerves were visible in the entirety. Thus the hyperintensities could be very well appreciated and the trauma localized. Compared to the other 3D DWIBS technique, nerve trauma was better visualized with 3D SHINKEI. Our results indicate that the SHINKEI sequence would increase the probability of nerve injury detection, associated muscle denervation, and is complementary to the conventional MR sequences. This can help in better surgical planning and hence warrants continued investigation on a larger patient cohort. Overall, a heavily T2 weighted 3D SHINKEI MRI sequence is clinically feasible to visualize brachial plexus in its entirety at 1.5T. Distally, subvoxel size nerves may suffer from blurring, and further work is warranted to optimize the signal spread for these fine nerves.

Declaration of patient consent

The authors certify that they have obtained all appropriate patient consent forms. In the form the patient(s) has/have given his/her/their consent for his/her/their images and other clinical information to be reported in the journal. The patients understand that their names and initials will not be published and due efforts will be made to conceal their identity, but anonymity cannot be guaranteed.

Financial support and sponsorship

This study was financially supported by Manipal Academy of Higher Education, Partial research fellowship from Philips Healthcare India.

Conflicts of interest

There are no conflicts of interest.

References

1. Bowen BC, Pattany PM, Saraf-Lavi E, Maravilla KR. The brachial plexus: Normal anatomy, pathology, and MR imaging. Neuroimaging Clin N Am 2004;14:59-85.
2. Orebaugh SL, Williams BA. Brachial plexus anatomy: Normal and variant. ScientificWorldJournal 2009;9:300-12.
3. Leinberry CF, Wehbé MA. Brachial plexus anatomy. Hand Clin 2004;20:1-5.
4. Thatte MR, Babhulkar S, Hiremath A. Brachial plexus injury in adults: Diagnosis and surgical treatment strategies. Ann Indian Acad Neurol 2013;16:26-33.
5. Kaiser R, Waldauf P, Ullas G, Krajcová A. Epidemiology, etiology, and types of severe adult brachial plexus injuries requiring surgical repair: Systematic review and meta-analysis. Neurosurg Rev 2020;43:443-52.
6. Malessy MJ, Pondaag W. Obstetric brachial plexus injuries. Neurosurg Clin N Am 2009;20:1-4.
7. van Geffen GJ, Moayeri N, Bruhn J, Scheffer GJ, Chan VW, Groen GJ. Correlation between ultrasound imaging, cross-sectional anatomy, and histology of the brachial plexus: A review. Reg Anesth Pain Med 2009;34:490-7.
8. Filler AG, Kliot M, Winn HR, Tsuruda JS, Hayes CE, Howe FA, *et al.* Magnetic resonance neurography. Lancet 1993;341:659-61.
9. Kasper JM, Wadhwa V, Scott KM, Rozen S, Xi Y, Chhabra A. SHINKEI – A novel 3D isotropic MR Neurography technique: Technical advantages over 3DIRTSE-based imaging. Eur Radiol 2015;25:1672-7.
10. Chhabra A, Zhao L, Carrino JA, Trueblood E, Koceski S, Shteriev F, *et al.* MR Neurography: Advances. Radiol Res Pract 2013;2013:809568.
11. Filler AG, Maravilla KR, Tsuruda JS. MR Neurography and muscle MR imaging for image diagnosis of disorders affecting the peripheral nerves and musculature. Neurol Clin 2004;22:643-82.
12. Chhabra A, Thawait GK, Soldatos T, Thakkar RS, Del Grande F, Chalian M, *et al.* High-resolution 3T MR neurography of the brachial plexus and its branches, with emphasis on 3D imaging. Am J Neuroradiol 2013;34:486-97.
13. Yoneyama M, Takahara T, Kwee TC, Nakamura M, Tabuchi T. Rapid high resolution MR neurography with a diffusion-weighted pre-pulse. Magn Reson Med Sci 2013;12:111-9.
14. Takahara T, Imai Y, Yamashita T, Yasuda S, Nasu S, Van Cauteren M. Diffusion weighted whole body imaging with background body signal suppression (DWIBS): Technical improvement using free breathing, STIR and high resolution 3D display. Radiat Med 2004;22:275-82.
15. Takahara T, Hendrikse J, Yamashita T, Mali WP, Kwee TC, Imai Y, *et al.* Diffusion-weighted MR Neurography of the brachial plexus: Feasibility

study. Radiology 2008;249:653-60.
16. Gasparotti R, Lodoli G, Meoded A, Carletti F, Garozzo D, Ferraresi S. Feasibility of diffusion tensor tractography of brachial plexus injuries at 1.5 T. Invest Radiol 2013;48:104-12.
17. Wang J, Yarnykh VL, Hatsukami T, Chu B, Balu N, Yuan C. Improved suppression of plaque-mimicking artifacts in black-blood carotid atherosclerosis imaging using a multislice motion-sensitized driven-equilibrium (MSDE) turbo spin-echo (TSE) sequence. Magn Reson Med 2007;58:973-81.
18. Wang J, Yarnykh VL, Yuan C. Enhanced image quality in black-blood MRI using the improved motion-sensitized driven-equilibrium (iMSDE) sequence. J Magn Reson Imaging 2010;31:1256-63.
19. Chhabra A, Andreisek G, Soldatos T, Wang KC, Flammang AJ, Belzberg AJ, *et al.* MR Neurography: Past, present, and future. Am J Roentgenol 2011;197:583-91.
20. Tagliafico A, Succio G, Neumaier CE, Serafini G, Ghidara M, Calabrese M, *et al*. MR imaging of the brachial plexus: Comparison between 1.5-T and 3-T MR imaging: Preliminary experience. Skeletal Radiol 2011;40:717-24.
21. Caranci F, Briganti F, La Porta M, Antinolfi G, Cesarano E, Fonio P, *et al.* Magnetic resonance imaging in brachial plexus injury. Musculoskelet Surg 2013;97:181-90.
22. Viallon M, Vargas MI, Jlassi H, Lövblad KO, Delavelle J. High-resolution and functional magnetic resonance imaging of the brachial plexus using an isotropic 3D T2 STIR (Short Term Inversion Recovery) SPACE sequence and diffusion tensor imaging. Eur Radiol 2008;18:1018-23.
23. Busse RF, Hariharan H, Vu A, Brittain JH. Fast spin echo sequences with very long echo trains: Design of variable refocusing flip angle schedules and generation of clinical T2 contrast. Magn Reson Med 2006;55:1030-7.
24. Cervantes B, Bauer JS, Zibold F, Kooijman H, Settles M, Haase A, *et al.* Imaging of the lumbar plexus: Optimized refocusing flip angle train design for 3D TSE. J Magn Reson Imaging 2016;43:789-99.
25. Busse RF, Brau AC, Vu A, Michelich CR, Bayram E, Kijowski R, *et al.* Effects of refocusing flip angle modulation and view ordering in 3D fast spin echo. Magn Reson Med 2008;60:640-9.
26. Klupp E, Cervantes B, Sollmann N, Treibel F, Weidlich D, Baum T, *et al.* Improved brachial plexus visualization using an adiabatic iMSDE-Prepared STIR 3D TSE. Clin Neuroradiol 2019;29:631-8.